Glycobiology vol. 20 no. 1 pp. 127–135, 2010
doi:10.1093/glycob/cwp155
Advance Access publication on October 12, 2009

An *Echinococcus multilocularis* coproantigen is a surface glycoprotein with unique *O*-gycosylation

Andreas J Hülsmeier[1,2,3], Peter Deplazes[2], Soraya Naem[4], Nariaki Nonaka[5], Thierry Hennet[3], and Peter Köhler[2]

[2]Institute of Parasitology, Winterthurerstrasse 266; [3]Institute of Physiology and Center for Integrative Human Physiology, University of Zurich, Winterthurerstrasse 190, Zurich, Switzerland; [4]Department of Pathobiology, College of Veterinary Medicine, Urmia University, Urmia, Iran; and [5]Laboratory of Veterinary Parasitic Diseases, Faculty of Agriculture, University of Miyazaki, Gakuen-kibanadai Nishi 1-1, Miyazaki 889-2192, Japan

Received on June 22, 2009; revised on September 22, 2009; accepted on September 25, 2009

A major surface constituent of *Echinococcus multilocularis* adult worms, referred to as an EmA9 antigen, was immunoaffinity purified and identified as a high-molecular-weight glycoconjugate. Labeling studies using the monoclonal antibody MAbEmA9 indicated that this antigen undergoes a regulated expression during the development from the larval to the adult parasite. Chemical modification of carbohydrate by periodate oxidation resulted in a reduced reactivity with antigen-specific antibodies. Non-reductive β-elimination of the purified molecule indicated the presence of *O*-linked glycans attached to threonine residues. Carbohydrate compositional analyses indicated the presence of *N*- and *O*-glycans with the ratio of carbohydrate to protein being 1.5:1 (w/w). *N*- and *O*-linked glycans were released by hydrazinolysis and analyzed as 2-aminobenzamide derivatized glycans by mass spectrometry together with HPLC and enzymatic sequencing. Novel linear *O*-linked saccharides with multiple β-HexNAc extensions of reducing end Gal were identified. *N*-Linked glycans were also detected with oligomannose and mono-, bi-, tri- and tetra-antennary-type structures, most of which were found to be core-fucosylated. Taken together, the results indicate that the EmA9 antigen is a glycoprotein located at the outer surface of the adult *E. multilocularis*. The observation that the EmA9 antigen expression is developmentally regulated suggests an involvement of this glycoprotein in the establishment of the parasite in its canine host.

Keywords: cestodes/hydrazinolysis/MALDI-TOF/TOF-MS/parasite worms

Introduction

The cestode *Echinococcus multilocularis* is the causative agent of human alveolar echinococcosis, a severe tumor-like parasitic disease that can be fatal if left untreated (Torgerson et al. 2008). In common with all other tapeworms, the parasite lacks an intestine and is covered by a syncytial tegument that mediates nutrient uptake and protects against the hosts' immune response. The life cycle of *E. multilocularis* comprises sexually mature, intestinal stages in the definitive host (carnivores), a free-living egg and the infective larval stage in the intermediate host (rodents) (Eckert and Deplazes 2004). Humans can be accidentally infected with the parasite by ingestion of eggs containing an oncosphere released with feces of the definitive host. Activated oncospheres penetrate the intestinal mucosa and enter via the blood circulation various host organs, most commonly the liver, where it further develops to the metacestode stage. This metacestode is built up of a multivesicular structure surrounded by an outer laminated layer and an inner germinal epithelium proliferating in an alveolar pattern. A major constituent of the laminated layer, the Em2(G11) antigen, has previously been defined as a mucin-type glycoprotein and suggested to play a major role in protecting the parasite from immune and other host defense reactions (Hülsmeier et al. 2002). Infection of the definitive host is caused by ingestion of metacestodes that develop within the small intestine into the adult worm.

In contrast to the metacestode laminated layer, scarce information is available about the structure and biological role of the tapeworm's adult stage surface constituents. The external surface coat is a highly dynamic structure with a short turnover rate. As has been shown for other helminths species (Hokke and Deelder 2001; Theodoropoulos et al. 2001; Thomas and Harn 2004), the outer membrane glycoconjugates of adult *E. multilocularis* may have crucial functions in host-parasite interactions, such as protecting the parasite by modulating the host's immune response. On the other hand, glycan determinants within surface and secreted glycoconjugates principally serve to initiate the immune responses against helminths in infected hosts (Nyame et al. 2004). Excretory/secretory antigens derived from axenic cultures of *E. multilocularis* pre-adult stages were successfully applied for the detection of specific antibodies in host sera, and antibodies raised against these antigens were used for the development of coproantigen tests (Deplazes et al. 1992; Morishima et al. 1999).

In the present work, we describe the identification of a diagnostically relevant antigen, immunoaffinity purified from *E. multilocularis* tegument preparations. The biochemical nature of this antigen was not understood previously, and here we provide the first description of a purification of this antigen. Biochemical and mass spectrometric characterization revealed the presence of a developmentally regulated, high-molecular-weight glycoprotein, modified by *N*-linked glycosylation and unique *O*-galactosyl saccharides linked to threonine. This work describes a new type of *O*-glycosylation in animals.

[1]To whom correspondence should be addressed: Tel: +41-44-6355104; Fax: +41-44-6356814; e-mail: a.j.hulsmeier@access.uzh.ch

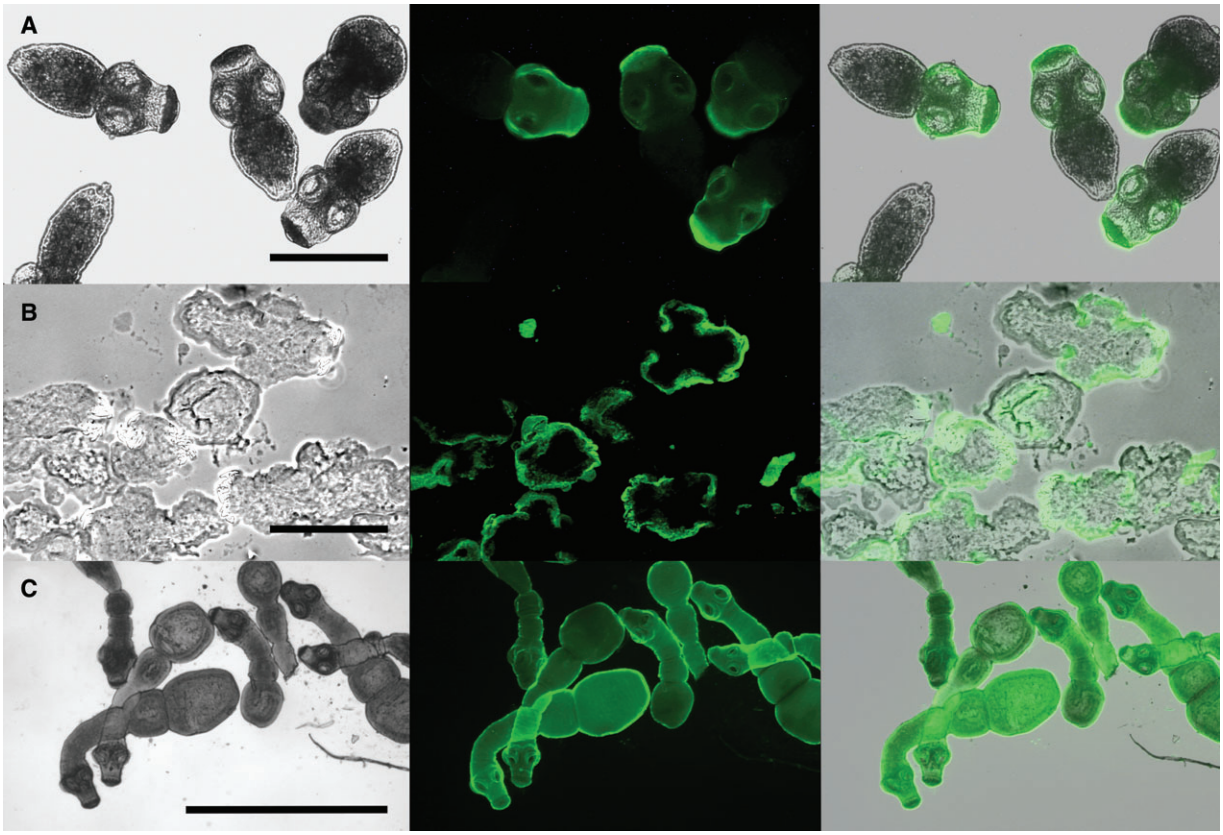

Fig. 1. Immunofluorescence staining of adult and larval stages (protoscoleces) of *E. multilocularis*. The monoclonal antibody EmA9 together with a FITC-conjugated anti-mouse antibody was used for staining. Left column: bright field microscopy. Middle column: immunofluorescence, FITC. Right column: overlay of left and middle column. Row (**A**): activated protoscoleces. Row (**B**): freeze fracture section of activated protoscoleces. Scale bar = 100 μm. Row (**C**): adult worms. Scale bar = 4 mm.

Results

E. multilocularis protoscoleces were isolated from infected *Meriones unguiculatus* voles and labeled with the monoclonal antibody MAbEmA9. Fluorescence detection was mediated by a FITC-conjugated anti-mouse monoclonal antibody. After activating the protoscoleces with acid-bile-pancreatin, a distinct staining of protoscoleces heads could be observed (Figure 1A). Specific antibody binding was not observed in preparations without the monoclonal antibody (conjugate control) or using an unrelated commercial mouse IgG3 antibody as control (data not shown). In freeze fracture sections, a surface location of the corresponding epitope was evident (Figure 1B). Interestingly, in adult *E. multilocularis* an intensive staining of the whole worm was observed (Figure 1C). These data indicate a regulated expression of the *E. multilocularis* EmA9 antigen during development from the larval stages to the adult worm.

The EmA9 antigen was purified from adult worm tegument preparations (Staebler et al. 2006) using an immuno-affinity column prepared with the MAbEmA9. Multiple column eluates were combined and subjected to size-exclusion chromatography. The antigen was detected by ELISA of aliquots from collected fractions. As shown in Figure 2, the antigen eluted from the size-exclusion column as a broad peak, indicating structural heterogeneity of the antigen. The main fractions eluting at 600 kDa were pooled for further analyses.

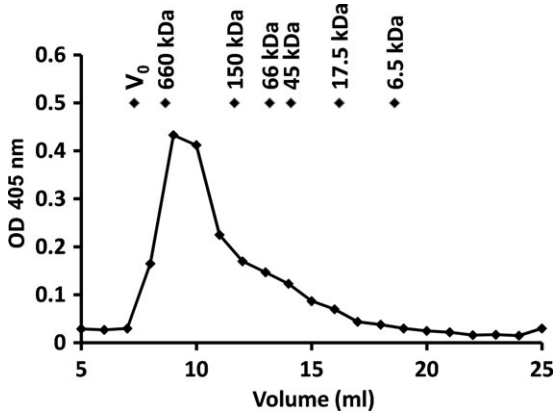

Fig. 2. Size-exclusion chromatography of the EmA9 antigen. One milliliter of fractions was collected and screened by sandwich- ELISA using the monoclonal antibody MAbEmA9. The elution positions of molecular mass standards are indicated with the corresponding molecular weight values.

Crude and purified EmA9 antigen preparations were subjected to sodium periodate oxidation and their reactivities with selected antibodies were assessed by ELISA. Upon oxidation, a clear decrease in signal intensity was observed with both polyclonal chicken anti-tegument antibodies and MAbEmA9,

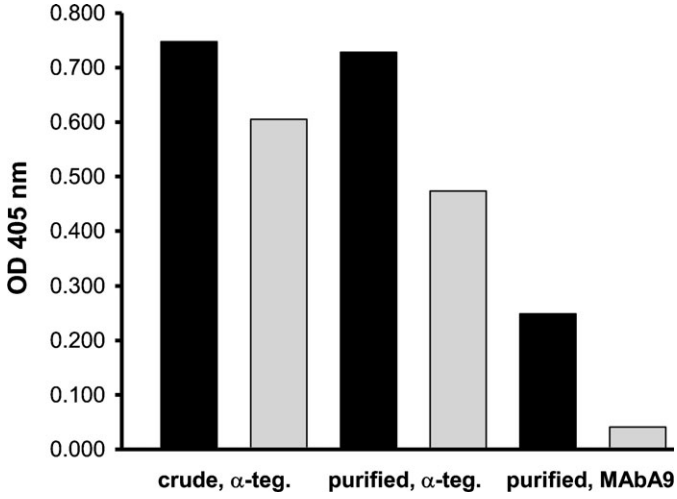

Fig. 3. Sandwich-ELISA analysis of the periodate-oxidized EmA9 antigen. Left: crude *E. multilocularis* tegumental antigen preparation detected with a polyclonal chicken anti-tegument antibody. Middle: the purified EmA9 antigen detected with a polyclonal chicken anti-tegument antibody. Right: the purified EmA9 antigen detected with the monoclonal antibody MAbEmA9. Black bars: without periodate oxidation; gray bars: antigens were subjected to periodate oxidation prior to ELISA analysis. Results are means of duplicate samples.

indicating that carbohydrates constitute major epitopes for these antibodies (Figure 3).

Nonreductive β-elimination of the purified EmA9 antigen resulted in a significant decrease of threonine in the amino acid composition, indicating the presence of *O*-linked glycans attached to the hydroxyamino acid (99.8% confidence, Table I). The amount of serine also appeared to be lowered, suggesting a second *O*-glycosylation type of the antigen. However, with a *p*-value of 0.1648 and a risk level of 0.05, the data do not support a significant decay of serine after β-elimination. Carbohydrate compositional analyses by high-performance liquid chromatography showed that the major carbohydrate constituents of the EmA9 antigen are derived from GlcNAc and Gal, together with significant amounts of Fuc, Man, and GalNAc. The molar ratio of Man:GlcNAc:GalNAc:Gal:Fuc was calculated to be 8:21:1:14:3, and the ratio of carbohydrate to protein was found to be 1.5:1 (w/w).

Glycans were released from the EmA9 antigen by hydrazinolysis under conditions, which release *O*-glycans as well as *N*-glycans (Patel et al. 1993). The liberated glycans were labeled with 2-aminobenzamide (2AB) and analyzed by NP-HPLC. Retention times were calibrated with 2AB-labeled dextran hydrosylate and converted into glucose units (GU) (Grubenmann et al. 2004). An unfractionated, 2AB-labeled sample aliquot was subjected to MALDI-TOF-MS and nine different saccharide compositions could be assigned (S2–S10, Table II). A comparison of fluorescence profiles of glycans released under *N*- and *O*-glycan liberating conditions with *O*-glycan only condition indicated the presence of *N*-glycosylation by the appearance of additional peaks, eluting >5 GU in the *N*- and *O*-glycan releasing condition (data not shown). For subsequent analyses, hydrazinolysis conditions liberating *N*- and *O*-glycans were used (Figure 4). GU values were directly assigned to mass determinations from collected NP-HPLC fractions for the saccharide compositions

Table I. Results of the amino acid and monosaccharide analyses of the EmA9 antigen

Component	Before β-elimination mol%[a]	After β-elimination mol%[a]	*p*-value
Asx	5.4 ± 0.68	4.6 ± 0.32	0.1256
Glx	5.3 ± 0.49	4.7 ± 0.53	0.2030
Ser	4.1 ± 0.07	3.3 ± 0.77	0.1648
His	1.1 ± 0.12	1.0 ± 0.09	0.6371
Gly	4.4 ± 0.63	4.1 ± 0.81	0.6283
Thr	5.6 ± 0.40	3.6 ± 0.28	0.0017
Ala/Arg	14.8 ± 1.33	11.7 ± 1.59	0.0621
Tyr	1.1 ± 0.10	1.0 ± 0.41	0.7001
Val	2.4 ± 0.20	2.4 ± 0.40	0.8924
Met	0.0	0.0	
Phe	1.5 ± 0.05	1.4 ± 0.15	0.6972
Ile	0.0	0.0	
Leu	4.2 ± 0.08	3.7 ± 0.61	0.1948
Lys	n.d.	n.d.	
Pro	2.9 ± 0.18	2.5 ± 0.35	0.1162
Man	7.9 ± 0.88		
GlcN	21.1 ± 1.31		
GalN	1.0 ± 0.20		
Gal	14.2 ± 1.53		
Fuc	2.9 ± 0.24		

[a]The data are background-corrected. Values are means ± SD, $n = 3$, n.d. = not detected. Statistical significance was calculated using the two-tailed Student's *t*-test model with the null hypothesis that the amounts of each amino acid are equal before and after β-elimination. *N*-Acetyl hexosamines were detected as their de-*N*-acetylated derivatives, respectively glucosamine (GlcN) and galactosamine (GalN).

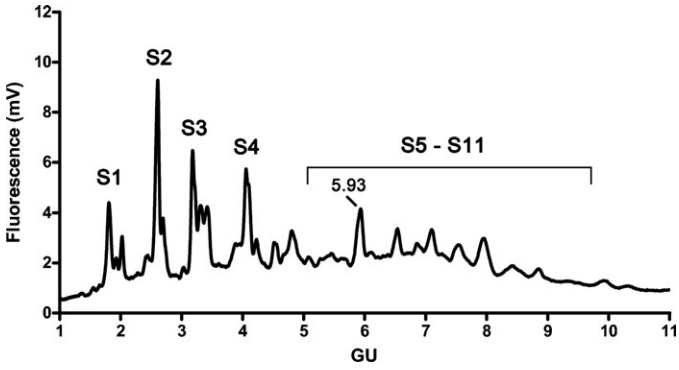

Fig. 4. NP-HPLC analysis of 2AB-labeled EmA9 *O*-linked and *N*-linked oligosaccharides. The retention times were externally calibrated with 2AB-labeled standard glucose oligomers and converted to glucose units (GU). Elution positions of the *O*-glycans S1–S4 and *N*-glycans S5–S11 are labeled. 5.93 GU corresponds to the elution time of a bi-antennary, core fucosylated *N*-glycan.

Hex1HexNAc2, Hex1HexNAc3, and Hex1HexNAc4 with 2.61 GU, 3.18 GU, and 4.06 GU, respectively. From the 2.61 GU and 3.18 GU, fractions collision-induced fragmentation spectra could be obtained by MALDI-TOF/TOF-MS, and the sequences HexNAc-HexNAc-Hex-2AB and HexNAc-HexNAc-HexNAc-Hex-2AB were assigned. Figure 5 shows the fragment spectrum of the saccharide S2 at 2.61 GU. The Y_1-fragment ion at *m/z* 323.1 corresponded to the 2AB-hexose and was also evident in the fragment spectrum corresponding to saccharide S3 (Table II). The Y_2-fragment ion at *m/z* 526.2 was the most

Table II. Summary of the data describing the *O*-linked structures S1-S4 and *N*-glycosylation of the EmA9 antigen

Designation	*m/z* meas.	*m/z* calc.	Δ Mass	Composition	Fragment ions (*m/z*)	JBBH	Reducing end	GU	Structure assignment
S1						+	Gal	1.81	HexNAcβ-Gal
S2	729.280	729.282	0.002	Hex1HexNAc2	226, 244, 305, 323, 351, 429, 447, 508, 526	+	Gal	2.61	HexNAcβ-HexNAcβ-Gal
S3	932.347	932.361	0.014	Hex1HexNAc3	226, 244, 323, 447, 526, 554, 729	+	Gal	3.18	HexNAcβ-HexNAcβ-HexNAcβ-Gal
S4	1135.431	1135.441	0.010	Hex1HexNAc4		+	Gal	4.06	HexNAcβ-HexNAcβ-HexNAcβ-HexNAcβ-Gal
S5	1377.472	1377.493	0.021	Hex5HexNAc2	226, 347, 364, 509, 567, 833, 874, 1036, 1215				Man5
S6	1402.518	1402.525	0.006	dHexHex3HexNAc3	226, 364, 510, 550, 713, 915, 1256				Mono-antennary, core Fuc
S7	1605.589	1605.604	0.015	dHexHex3HexNAc4	364, 510, 538, 567, 713, 741, 915, 931, 1118, 1136, 1402, 1459				Bi-antennary, core Fuc
S8	1751.657	1751.662	0.005	dHex2Hex3HexNAc4	364, 567, 713, 915, 1118, 1264, 1403				Bi-antennary, 1 x Fuc, core Fuc
S9	1767.657	1767.657	0.000	dHexHex4HexNAc4	1264, 1280, 1462, 1621				Bi-antennary, 1 Gal, 1 Fuc
S10	1808.665	1808.684	0.019	dHexHex3HexNAc5	226, 364, 388, 510, 550, 713, 753, 915, 1118, 1321, 1402				Tri-antennary, core Fuc
S11	2012.117	2011.763	0.354	dHexHex3HexNAc6	364, 567, 713, 915, 1321, 1524, 1606, 1809				Tetra-antennary, core Fuc

MALDI-TOF/TOF-MS data: *m/z* meas.: measured values; *m/z* calc.: theoretical values; Δ mass: *m/z* value deviation measured from theoretical values; JBBH: Jack bean beta-*N*-acetyl-hexosaminidase susceptibility, + susceptible to JBBH; reducing end saccharide analysis of JBBH digestion products subjected to RP-HPLC; GU: glucose units determined by NP-HPLC.

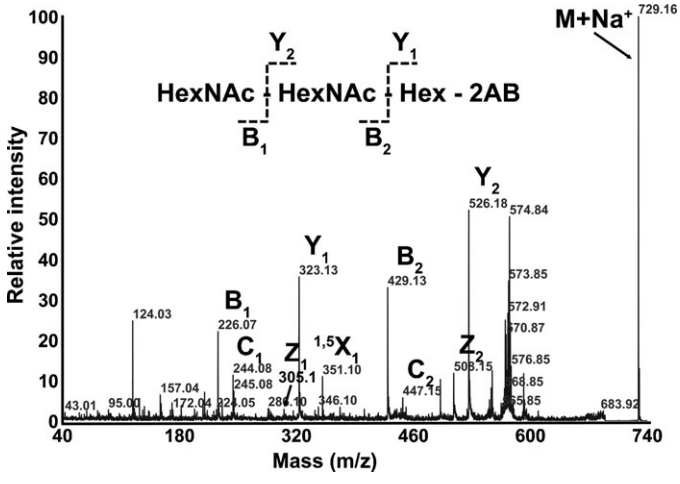

Fig. 5. MALDI-TOF/TOF-MS of the *O*-glycan S2. The fragment spectrum obtained from the peak fractions eluting at 2.61 GU (see Figure 4) together with the assigned saccharide structure is shown. The main fragment ions are labeled; $M+Na^+$: precursor ion.

intense fragment ion in the spectrum and described the disaccharide HexNAc-Hex-2AB. On the other hand, the abundant B_2-fragment ion at *m/z* 492.1 described the HexNAc-HexNAc disaccharide. These two ions can only be generated from a linear structure, suggesting the sequence HexNAc-HexNAc-Hex-2AB for saccharide S2. Apparent Z_1-, Z_2-, C_1-, and C_2-type ions complemented this assignment.

Peak fractions at 1.81 GU, 2.61 GU, 3.18 and 4.06 GU corresponding to S1–S4 were digested with JBBH and rechromatographed by NP-HPLC (Figure 6). Susceptibility to the Jack Bean enzyme could be observed with all four fractions, indicating β-anomericity for the HexNAc constituents and confirming the sequence assignments obtained from MALDI-TOF/TOF-MS. 2AB-labeled chitobiose was treated in parallel with the peak fractions and was completely converted to 2AB-GlcNAc (data not shown). Reverse-phase chromatography of the JBBH-treated fractions showed a co-elution of the reducing end hexose with 2AB-galactose, indicating that galactose is the reducing end constituent in the EmA9 *O*-linked glycans. As shown in Figure 7, 2AB-galactose derived from saccharide S2 was clearly separated from 2AB-mannose, an alternative candidate for the reducing end hexose (compare with Table I).

In unfractionated 2AB-labeled sample aliquots, *m/z* values correlating to possible *N*-glycan structures were also acquired (data not shown). However, after NP-HPLC separation, fragment spectra could not be acquired from the collected peak fractions, thus preventing a direct GU and sequence assignment to the *m/z* values. Therefore, the NP-HPLC fractions

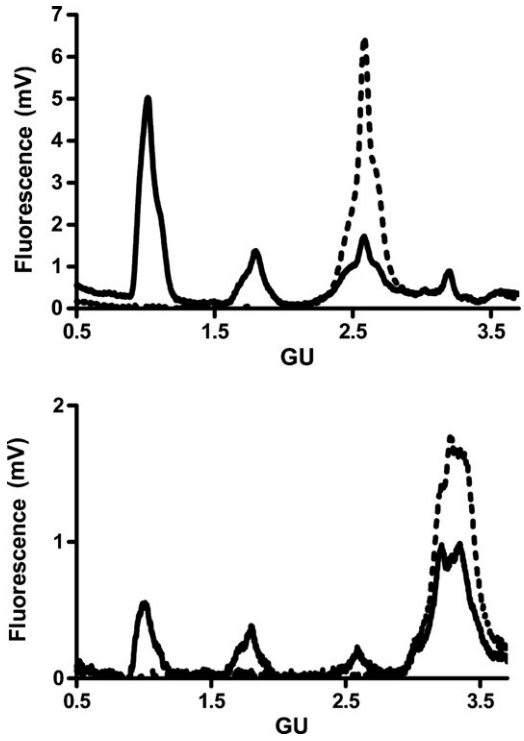

Fig. 6. Jack bean β-*N*-acetylhexosaminidase (JBBH) digestion. NP-HPLC of fractions corresponding to S2 (top panel) and S3 (bottom panel) was re-chromatographed after JBBH digestion (continuous line) or without JBBH digestion (dotted line). Retention times are given in GU (see Figure 4).

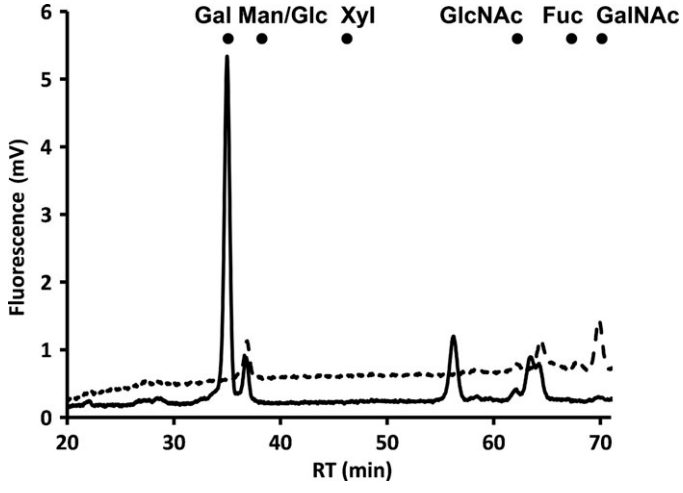

Fig. 7. Reducing-end-saccharide analysis. The NP-HPLC peak fractions corresponding to S2 before (dotted line) and after JBBH digestion were analyzed by RP-HPLC. The elution positions of authentic 2AB-labeled monosaccharides are marked with dots.

corresponding to the elution times of potential *N*-glycans (i.e., >4.2 GU) were pooled, desalted with porous graphitized silica, concentrated and re-analyzed by MALDI-TOF/TOF-MS. Fragment spectra were acquired from oligomannose 5 (Man5) and mono-, bi-, tri- and tetra-antennary-type *N*-glycan structures (Table II). Apart from the Man5 glycan, all *N*-glycans contained

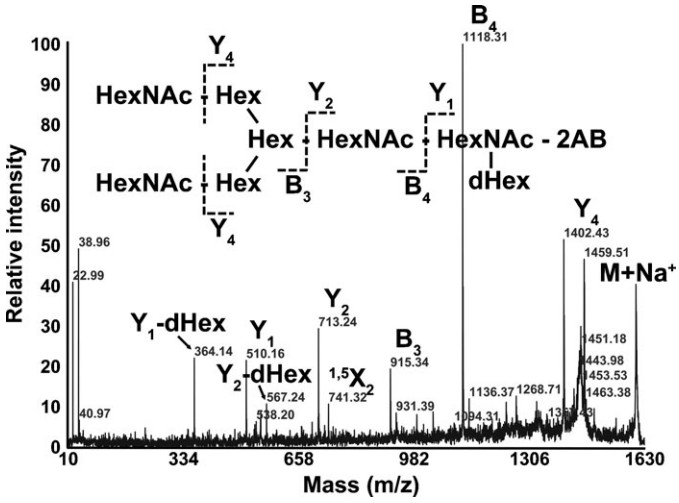

Fig. 8. MALDI-TOF/TOF-MS of the *N*-glycan S7. The fragment spectrum of the precursor ion at *m/z* 1605.589 obtained from the pooled fractions of S5–S11 (see Figure 4) together with the assigned *N*-glycan structure is shown. The main fragment ions are labeled; $M+Na^+$: precursor ion.

one or two fucoses and for all but structure S9, core fucosylation was evidenced by the presence of fragment ions corresponding to dHex-modified Y_1 and/or Y_2 fragments (Figure 8). The second fucose in saccharide S8 might be attached to a terminal HexNAc, as indicated by the presence of a B_4 +dHex fragment ion at *m/z* 1264 (Table II). In addition, fragment spectra from a core fucosylated, tetra-antennary *N*-glycan at *m/z* 2012 could be acquired (S11, Table II). The presence of bisecting *N*-glycans in the acquired spectra cannot be excluded. However, the fluorescence peak at 5.93 GU could be assigned to structure S7 and would be in good agreement with 5.90 and 5.93 GU values described before for bi-antennary core fucosylated *N*-glycans (see Figure 4) (Rudd et al. 1999, 2001).

Discussion

In recent years, a large amount of structural data on helminth-derived glycans has become available due to the application of sensitive and sophisticated analytical techniques primarily HPLC, NMR, and mass spectrometry (Huang et al. 2001). The diverse array of defined oligosaccharide elements includes both *N*- and *O*-glycans of surface and secreted glycoconjugates most of which induce strong antibody responses in parasitized hosts (Khoo and Dell 2001). The glycans in helminth glycoproteins possess structures resembling in many ways those found in higher organisms, but frequently these molecules are specifically modified resulting in a range of novel carbohydrate architectures (Hokke and Deelder 2001). The present study describes the glycan structures of a surface antigen expressed by the adult stages of *E. multilocularis*. This antigen is recognized by the monoclonal antibody EmA9 that has been used as a tool in coproantigen diagnosis of canine echinococcosis (Nonaka et al. 1998). A strong surface expression of the EmA9 antigen could be detected in the adult stages of *E. multilocularis*, whereas only the heads were stained in activated protoscoleces (Figure 1). This is the first observation of the EmA9 epitope in the larval life cycle stage, indicating a developmentally regulated expression

of this antigen. The clear decrease in the immunoreactivity of the EmA9 antigen following periodate oxidation confirmed an association of its antigenic character with glycan structures. Subsequent chemical and statistical analyses showed that the majority of these glycans are O-linked to threonine residues of the peptide backbone. GlcNAc and Gal are the dominant sugar constituents with Gal at the reducing termini. Gal-α-Ser/Thr linkages, extended with one or two alpha-linked Gal, have been reported to occur in cuticle collagens of free living earth- and clamworms (Spiro 2002). The molar percentage of Gly in the amino acid composition of the purified EmA9 antigen speaks against the possibility of a collagen domain in the antigen. Additional peptide sequencing and nucleotide cloning experiments would be required to unravel the identity of the peptide backbone. Further, the anomericity of the Gal to Thr linkage in the EmA9 antigen was not determined. Gal linked in β-anomericity to a peptide backbone has only been described in linkages to hydroxylysine or hydroxyproline (Spiro 2002), and a Gal-β-Thr linkage in the EmA9 antigen would establish a novel type of *O*-glycosylation core structure. Such investigations require large-scale purification of the EmA9 antigen and corresponding glycopeptides followed by enzymatic deglycosylation analyses. *O*-Linked Gal appears generally much less widely dispersed in nature than mucin-type GalNAc-Ser/Thr or the GlcNAc-Ser/Thr linkage. Recently, a single *O*-linked tri-saccharide structure with galactose at the reducing end and elongated with GlcNAc and terminal Gal was described in *Schistosoma mansoni*, whereas the majority of *O*-glycosylation was attributed to mucin-type glycosylation (Jang-Lee et al. 2007). GalNAc-Ser/Thr linkages were not found in the EmA9 antigen, and this glycoprotein differs significantly in its glycoconjugate composition compared to the mucin-type *O*-glycosylation of the Em2(G11) surface glycoprotein expressed by the *E. multilocularis* larval stage. An unusual feature of the EmA9 antigen glycoprotein is the presence of β-HexNAc extensions of reducing end Gal residues. By correlating the high abundance of GlcNAc in the carbohydrate compositional analyses with the major fluorescence peaks of the 2AB-labeled EmA9 antigen saccharides, it can be suggested that β-GlcNAc residues are extending the reducing end Gal residues. To our knowledge, these *O*-linked glycoconjugate structures do not have precedence in any other species described in the literature. *N*-Linked glycans have also been detected with mono-, bi-, tri- and tetra-antennary-type structures, most of which were found to be core-fucosylated and not distinguished by novel structural features. The terminal fucose residue in the *N*-glycan structure S8 might mimik blood group Lewis^a or Lewis^x motives and mediate cellular interactions in the host intestine in support of the manifestation of the parasite infection. Lewis^x epitope bearing glycoconjugates have been described in detergent extracts of the parasitic nematode *Dictyocaulus viviparus* and in antigens derived from parasitic trematodes *Schistosoma* spp. and were implicated in immunomodulatory host responses during establishment of schistosome infection in mice (Velupillai and Harn 1994; Haslam et al. 2000; Nyame et al. 2004).

Previously, a major surface antigen, stage-specifically expressed by the larval stage of *E. multilocularis*, has been characterized as a mucin-type *O*-glycosylated protein (Hülsmeier et al. 2002). The glycans of this Em2(G11) antigen were found to contain novel linear and branched oligosaccharide structures that differ from the adult stage antigen in containing Gal and GalNAc as major constituents with GalNAc being the sole reducing end saccharide. Furthermore, in contrast to the adult stage EmA9 antigen, N-linked glycosylation was not found in the larval stage Em2(G11) antigen (Hülsmeier et al. 2002). Other studies have shown that the adult stages of the dog tapeworm *E. granulosus* also contain epitopes recognized by the MAbEmA9 (Malgor et al. 1997), and indirect methods using lectin binding have identified carbohydrate structures in the tegument and other tissues of this closely related parasite with Gal, GalNAc, and Man as major glycan constituents (Casaravilla et al. 2003). A similar carbohydrate composition pattern appears to be present in other tapeworms including *Taenia taeniaeformis* and *Hymenolepis diminuta*, but the structures of these glycans have also not been defined (Casaravilla et al. 2003). The most extensively and best studied helminth antigenic glycan structures are those carried by schistosomes. These parasites synthesize *O*-glycans ranging from short mucin-type saccharides to highly complex *O*-glycans containing multifucosylated unusual structural elements (Hokke and Deelder 2001). In addition, various stages of this parasite express glycoproteins carrying both, simple and more complex multi-antennary *N*-linked glycans. Many of this great variety of structures have been chemically defined. Interestingly, the glycans of *Echinococcus* and other cestode antigens show some resemblance to the cancer-associated simple *O*-glycosylated antigens (Alvarez Errico et al. 2001). Glycoproteins containing these truncated *O*-glycans, such as the Tn (αGalNAc-*O*-R), TF (βGal1,3-αGalNAc-*O*-R), and Tk [GlcNAcβ1-6(GlcNAcβ1-3)Gal-*O*-R] structures, seem to be widely expressed in helminths (Osinaga 2007; Ubillos et al. 2007).

The precise physiological functions of helminth glycoconjugates are still unclear. Previous studies have shown that immune responses against various helminth species in infected hosts are mainly directed toward glycan structures of surface or secreted glycoconjugates (Ferreira et al. 2000; Nyame et al. 2004). These macromolecules are therefore believed to play critical roles in host-parasite interactions including host recognition, attachment to host tissues, protection of vital tegumental structures, and immune evasion. Like most of the helminth glycoconjugates, the biological role of the EmA9 antigen in the host-parasite interplay is unknown, but the observation that this molecule is developmentally upregulated in the maturing larvae suggests that it plays an important role in the establishment of the parasite in its host and success of the infection. The present study may be a first step toward a better understanding of the interaction between the tapeworm EmA9 antigen and its canine host at the molecular level. The striking differences in glycosylation of the adult versus larval stage antigens reflect an adaptation to the dramatic environmental changes from the definite (canine, small intestine) to the intermediate (rodent, liver) host during the life cycle of *E. multilocularis*.

Material and methods

Immunofluerescence labeling of larval stages and adult worms

Adult stage worms were collected from naturally infected foxes (Deplazes et al. 1999) and conserved with 5% buffered formalin until further processing. *E. multilocularis* larval stages (protoscoleces) were isolated from infected *Meriones unguiculatus* voles and used for immunnofluorescence staining after acid-bile-pancreatin-mediated activation in liquid

preparations or in freeze fracture sections (Thompson et al. 1990). Protoscoleces were stained with and without prior formalin fixation and no differences could be observed in the staining pattern. Formalin-fixed specimens were treated with 50 mM ammonium chloride and 5% fetal calf serum (FCS) in PBS for 20 min and 30 min at room temperature, respectively, and subsequently incubated with the IgG3 monoclonal antibody MAbEmA9 (5 μg/mL PBS) (Kohno et al. 1995) or with 5 μg/mL PBS of an unrelated purified IgG3 MAb (I3784, Sigma-Aldrich, St. Louis, MO) for 1 h at 37°C. The specimens were washed twice with 5% FCS in PBS and incubated with an anti-mouse FITC conjugated secondary antibody (goat anti-mouse IgA, IgG, IgM, F 1010, Sigma), diluted 1:500 in 5% FCS in PBS, for 1 h at 37°C. Then, the specimens were washed once with 5% FCS in PBS and directly examined by fluorescence microscopy (in all experiments conjugate controls without MAbs were performed to confirm specific antibody reactions).

Size-exclusion chromatography

The *E. multilocularis* EmA9 antigen was immunoaffinity purified using the monoclonal antibody MAbEmA9 coupled with CNBr-activated Sepharose. The column was prepared according to the manufacturers' instructions and the eluted antigen was subjected to Superdex 200 HR (GE Healthcare) gel-filtration as described (Hülsmeier et al. 2002).

Amino acid analysis and carbohydrate compositional analyses

Amino acid analysis and nonreductive β-elimination were performed as previously described (Hülsmeier et al. 2002). Changes in amino acid composition were statistically validated using the two-tailed Student's *t*-test model with a risk level of $\alpha = 0.05$ and a degree of freedom calculated as $df = (n_{\text{before}} + n_{\text{after}}) - 2 = 4$.

The *t*-values were calculated with $t = \frac{\bar{X}_{\text{before}} - \bar{X}_{\text{after}}}{\sqrt{\frac{SD^2_{\text{before}}}{n_{\text{before}}} + \frac{SD^2_{\text{after}}}{n_{\text{after}}}}}$.

Carbohydrate analyses were carried out by reversed-phase HPLC of 1-phenyl-3-methyl-5-pyrazolone derivatized monosaccharides (Honda et al. 1989; Fu and O'Neill 1995). Aliquots of purified EmA9 antigen preparation were pre-mixed with 1 nmol lyxose internal standard each. For each batch of samples, two standards of 0.5–1 nmol of mannose (Man), lyxose, *N*-acetylglucosamine (GlcNAc), *N*-acetylgalactosamine (GalNAc), glucose, galactose (Gal), xylose, and fucose were prepared. The antigen and standard samples were hydrolyzed in 100 μL of 2 M trifluoroacetic acid (TFA) for 4 h at 100°C in a 0.8 mL crimp top glass vial. The samples were dried in a rotary evaporator and washed with 100 μL of 2-propanol followed by evaporation. Then, 20 μL of 0.5 M 1-phenyl-3-methyl-5-pyrazolone in methanol and 20 μL of 0.3 M NaOH were added and the samples were incubated for 40 min at 70°C. After cooling to room temperature, the samples were neutralized with 10 μL of 0.6 M HCl and vacuum dried to remove methanol. The samples were re-dissolved in 100 μL water and extracted four times with 200 μL dibutyl ether. The upper organic phase was discarded and 10–60% of the sample were analyzed by reversed-phase HPLC using a Vydac 208TP53, 300 Å, C8, 3.2 × 250 mm column, and UV detection at 245 nm. Buffer A was 10% acetonitrile in 50 mM sodium acetate, pH 4.7, buffer B was 25% acetonitrile in 50 mM sodium acetate, pH 4.7, and buffer C was 80% acetonitrile in water.

The following program was used.

Time (min)	% Buffer A	% Buffer B	% Buffer C	Flow (mL/min)
0.0	100			1.0
8.0	100			0.5
10.0	80	20		
48.0		100		
53.0		100		
53.1			100	
56.0			100	
56.1	100			
61.0	100			

Molecular relative response factors versus the lyxose internal standard were calculated for each monosaccharide and the amounts of each monosaccharide in the sample were calculated with respect to the response factor in relation to the lyxose internal standard in the sample.

Periodate oxidation

Aliquots of crude or purified EmA9 antigen fractions were incubated in 50 mM sodium meta-periodate in PBS in the dark for 3 h at room temperature. An equal volume of freshly prepared 1 M sodium borohydride was added, and the reaction mixture was incubated for 1 h at room temperature. The antigen preparations were dialyzed against PBS and subjected to ELISA antigen detection as described (Deplazes et al. 1992).

Hydrazinolysis

The purified EmA9 antigen was extensively dialyzed against 0.1% TFA at 4°C, lyophilized, and subjected to hydrazinolysis for 4 h at 95°C as described (Patel et al. 1993). For re-*N*-acetylation of hexosamines, acetic acid anhydride was added to ice cold, saturated sodium bicarbonate dissolved reaction products. Reducing end acetylations were removed by passage through 3 mL Dowex AG50 resin and incubation in 2 mL of 1 mM copper acetate in 1 mM acetic acid for 1 h at room temperature. Liberated oligosaccharides were purified by passage through 2 mL ODS resin over 1 mL Dowex AG50 and subjected to 2-amino benzamide (2AB) labeling and normal-phase (NP) HPLC analyses as described earlier (Grubenmann et al. 2004).

Mass spectrometry

The MALDI matrix was prepared by suspending 10 mg DHB in 1 mL of 50% acetonitrile, containing 1 mM NaCl. The sample and matrix were mixed on the MALDI plate at a ratio of 1:1 and allowed to dry at room temperature. The dried spots were re-crystallized by applying <0.1 μL ethanol. MALDI mass spectra were recorded in positive ion mode, using an Applied Biosystems 4700 Proteomics Analyzer (Applied Biosystems). Averages of 2000–5000 laser shots were used to obtain MS/MS spectra. The collision energy was set at 1 kV and the air pressure inside the collision cell was set at 2×10^{-6} Torr.

Jack bean β-N-acetylhexosaminidase (JBBH) digestions

Two equal aliquots per pooled peak fractions collected from NP-HPLC were dried by rotary evaporation. One tube was subjected to JBBH (Prozyme) digestion and the other tube was incubated in the digestion buffer only. Enzymatic digestion was carried out

in 20 μL volumes of 0.1 M sodium acetate buffer, pH 5.5, and 10 U JBBH per mL. The digestion mixture was overlaid with 10 μL mineral oil and incubated at 37°C for 16 h. The reaction products were re-analyzed by NP-HPLC.

Reducing end saccharide analysis

The 2AB-saccharide fractions obtained after JBBH digestion were applied to reverse-phase chromatography on a Hypersil ODS column, 4.6 × 150 mm, 3 μm particle size (Thermo Electron Corporation) and eluted using a trinary solvent gradient system at a flow rate of 0.8 mL/min at 40°C. Buffer A was 50 mM sodium acetate, pH 4.7, buffer B was buffer A with 10% acetonitrile, and buffer C was 100% acetonitrile.

The following program was used.

Time (min)	% Buffer A	% Buffer B	% Buffer C
0.0	100		
10.0	100		
70.0	85	15	
80.0	20		80
90.0	20		80
100.0	100		
120.0	100		

The elution positions of authentic 2AB-monosaccharide derivatives were determined prior and post-sample application (Chiba et al. 1997).

Funding

This work was supported by the University of Zurich, Switzerland.

Acknowledgements

We thank Isabell Tanner and Cornelia Spycher, Institute of Parasitology Zurich for the excellent laboratory support and the Functional Genomic Center Zurich (FGCZ), Switzerland, and Dr. P. Gehrig, FGCZ for their support with the MALDI-TOF-TOF-mass spectrometer

Abbreviations

MAb, monoclonal antibody; HexNAc, *N*-acetylhexosamine; Hex, hexose; Gal, galactose; Man, mannose; GlcNAc, *N*-acetylglucosamine; GalNAc, *N*-acetylgalactosamine; MALDI-TOF/TOF-MS, matrix-assisted laser-desorption/ionisation time-of-flight tandem mass spectrometry; JBBH, Jack bean β-*N*-acetylhexosaminidase; NP-HPLC, normal-phase HPLC; 2AB, 2-amino benzamide; GU, glucose units.

References

Alvarez Errico D, Medeiros A, Miguez M, Casaravilla C, Malgor R, Carmona C, Nieto A, Osinaga E. 2001. *O*-Glycosylation in *Echinococcus granulosus*: Identification and characterization of the carcinoma-associated Tn antigen. *Exp Parasitol.* 98:100–109.

Casaravilla C, Malgor R, Carmona C. 2003. Characterization of carbohydrates of adult *Echinococcus granulosus* by lectin-binding analysis. *J Parasitol*. 89:57–61.

Chiba A, Matsumura K, Yamada H, Inazu T, Shimizu T, Kusunoki S, Kanazawa I, Kobata A, Endo T. 1997. Structures of sialylated *O*-linked oligosaccharides of bovine peripheral nerve alpha-dystroglycan. The role of a novel *O*-mannosyl-type oligosaccharide in the binding of alpha-dystroglycan with laminin. *J Biol Chem*. 272:2156–2162.

Deplazes P, Alther P, Tanner I, Thompson RC, Eckert J. 1999. *Echinococcus multilocularis* coproantigen detection by enzyme-linked immunosorbent assay in fox, dog, and cat populations. *J Parasitol*. 85:115–121.

Deplazes P, Gottstein B, Eckert J, Jenkins DJ, Ewald D, Jimenez-Palacios S. 1992. Detection of *Echinococcus* coproantigens by enzyme-linked immunosorbent assay in dogs, dingoes and foxes. *Parasitol Res*. 78:303–308.

Eckert J, Deplazes P. 2004. Biological, epidemiological, and clinical aspects of echinococcosis, a zoonosis of increasing concern. *Clin Microbiol Rev*. 17:107–135.

Ferreira AM, Irigoin F, Breijo M, Sim RB, Diaz A. 2000. How Echinococcus granulosus deals with complement. *Parasitol Today*. 16:168–172.

Fu D, O'Neill RA. 1995. Monosaccharide composition analysis of oligosaccharides and glycoproteins by high-performance liquid chromatography. *Anal Biochem*. 227:377–384.

Grubenmann CE, Frank CG, Hülsmeier AJ, Schollen E, Matthijs G, Mayatepek E, Berger EG, Aebi M, Hennet T. 2004. Deficiency of the first mannosylation step in the *N*-glycosylation pathway causes congenital disorder of glycosylation type Ik. *Hum Mol Genet*. 13:535–542.

Haslam SM, Coles GC, Morris HR, Dell A. 2000. Structural characterization of the *N*-glycans of *Dictyocaulus viviparus*: Discovery of the Lewis(x) structure in a nematode. *Glycobiology*. 10:223–229.

Hokke CH, Deelder AM. 2001. Schistosome glycoconjugates in host-parasite interplay. *Glycoconj J*. 18:573–587.

Honda S, Akao E, Suzuki S, Okuda M, Kakehi K, Nakamura J. 1989. High-performance liquid chromatography of reducing carbohydrates as strongly ultraviolet-absorbing and electrochemically sensitive 1-phenyl-3-methyl-5-pyrazolone derivatives. *Anal Biochem*. 180:351–357.

Huang HH, Tsai PL, Khoo KH. 2001. Selective expression of different fucosylated epitopes on two distinct sets of *Schistosoma mansoni* cercarial *O*-glycans: Identification of a novel core type and Lewis X structure. *Glycobiology*. 11:395–406.

Hülsmeier AJ, Gehrig PM, Geyer R, Sack R, Gottstein B, Deplazes P, Köhler P. 2002. A major *Echinococcus multilocularis* antigen is a mucin-type glycoprotein. *J Biol Chem.* 277:5742–5748.

Jang-Lee J, Curwen RS, Ashton PD, Tissot B, Mathieson W, Panico M, Dell A, Wilson RA, Haslam SM. 2007. Glycomics analysis of *Schistosoma mansoni* egg and cercarial secretions. *Mol Cell Proteomics.* 6:1485–1499.

Khoo KH, Dell A. 2001. Glycoconjugates from parasitic helminths: Structure diversity and immunobiological implications. *Adv Exp Med Biol*. 491:185–205.

Kohno H, Sakai H, Okamoto M, Ito M, Oku Y, Kamiya M. 1995. Development and characterization of murine monoclonal antibodies to *Echinococcus multilocularis* adult worms and its use for the coproantigen detection. *Japan J Parastiol*. 44:404–412.

Malgor R, Nonaka N, Basmadjian I, Sakai H, Carambula B, Oku Y, Carmona C, Kamiya M. 1997. Coproantigen detection in dogs experimentally and naturally infected with *Echinococcus granulosus* by a monoclonal antibody-based enzyme-linked immunosorbent assay. *Int J Parasitol*. 27:1605–1612.

Morishima Y, Tsukada H, Nonaka N, Oku Y, Kamiya M. 1999. Evaluation of coproantigen diagnosis for natural *Echinococcus multilocularis* infection in red foxes. *Japan J Vet Res.* 46:185–189.

Nonaka N, Tsukada H, Abe N, Oku Y, Kamiya M. 1998. Monitoring of *Echinococcus multilocularis* infection in red foxes in Shiretoko, Japan, by coproantigen detection. *Parasitology*. 117(Pt 2):193–200.

Nyame AK, Kawar ZS, Cummings RD. 2004. Antigenic glycans in parasitic infections: Implications for vaccines and diagnostics. *Arch Biochem Biophys*. 426:182–200.

Osinaga E. 2007. Expression of cancer-associated simple mucin-type *O*-glycosylated antigens in parasites. *IUBMB Life*. 59:269–273.

Patel T, Bruce J, Merry A, Bigge C, Wormald M, Jaques A, Parekh R. 1993. Use of hydrazine to release in intact and unreduced form both *N*- and *O*-linked oligosaccharides from glycoproteins. *Biochemistry*. 32:679–693.

Rudd PM, Colominas C, Royle L, Murphy N, Hart E, Merry AH, Hebestreit HF, Dwek RA. 2001. A high-performance liquid chromatography based strategy

for rapid, sensitive sequencing of *N*-linked oligosaccharide modifications to proteins in sodium dodecyl sulphate polyacrylamide electrophoresis gel bands. *Proteomics*. 1:285–294.

Rudd PM, Wormald MR, Harvey DJ, Devasahayam M, McAlister MS, Brown MH, Davis SJ, Barclay AN, Dwek RA. 1999. Oligosaccharide analysis and molecular modeling of soluble forms of glycoproteins belonging to the Ly-6, scavenger receptor, and immunoglobulin superfamilies expressed in Chinese hamster ovary cells. *Glycobiology*. 9:443–458.

Spiro RG. 2002. Protein glycosylation: Nature, distribution, enzymatic formation, and disease implications of glycopeptide bonds. *Glycobiology*. 12:43R–56R.

Staebler S, Grimm F, Glaus T, Kapel CM, Haller M, Hasler A, Hanosset R, Deplazes P. 2006. Serological diagnosis of canine alveolar echinococcosis. *Vet Parasitol*. 141:243–250.

Theodoropoulos G, Hicks SJ, Corfield AP, Miller BG, Carrington SD. 2001. The role of mucins in host-parasite interactions: Part II. Helminth parasites. *Trends Parasitol*. 17:130–135.

Thomas PG, Harn DA Jr. 2004. Immune biasing by helminth glycans. *Cell Microbiol*. 6:13–22.

Thompson RC, Deplazes P, Eckert J. 1990. Uniform strobilar development of *Echinococcus multilocularis* in vitro from protoscolex to immature stages. *J Parasitol*. 76:240–247.

Torgerson PR, Schweiger A, Deplazes P, Pohar M, Reichen J, Ammann RW, Tarr PE, Halkik N, Müllhaupt B. 2008. Alveolar echinococcosis: From a deadly disease to a well-controlled infection. Relative survival and economic analysis in Switzerland over the last 35 years. *J Hepatol*. 49:72–77.

Ubillos L, Medeiros A, Cancela M, Casaravilla C, Saldana J, Dominguez L, Carmona C, Le Pendu J, Osinaga E. 2007. Characterization of the carcinoma-associated Tk antigen in helminth parasites. *Exp Parasitol*. 116:129–136.

Velupillai P, Harn DA. 1994. Oligosaccharide-specific induction of interleukin 10 production by B220+ cells from schistosome-infected mice: A mechanism for regulation of CD4+ T-cell subsets. *Proc Natl Acad Sci USA*. 91:18–22.